

Longitudinal Jet Cross Sections in Order α_s^2

B. Lampe and G. Kramer

II. Institut für Theoretische Physik der Universität Hamburg, Luruper Chaussee 149,
D-2000 Hamburg 50, Federal Republic of Germany

Dedicated to the memory of Kurt Symanzik

Abstract. We calculate the cross section for $e^+e^- \rightarrow 3$ jets for longitudinally polarized virtual photons up to order α_s^2 in the quark-gluon coupling.

1. Introduction

The cross sections for the production of 2, 3, and 4 jets in e^+e^- annihilation as measured at PETRA and PEP have given us useful information about the quark-gluon dynamics as described by QCD [1]. So, for example, the 3-jet cross section has been used in various ways for determining the quark-gluon coupling constant in the perturbative region [2].

Considering also the orientation of the jets with respect to the direction of the incoming beam the 3-jet cross section depends in general on three independent cross sections σ_U , σ_L , σ_T , and σ_I , where U , L , T , and I label the polarization of the ingoing virtual photon [3]. These polarization dependent cross sections which fully determine the jet angular correlations with respect to the incoming electron beam in $e^+e^- \rightarrow q\bar{q}g$ are known up to order α_s [3]. So far only the angular averaged 3-jet cross section $\sigma_{U+L} = \sigma_U + \sigma_L$ has been measured. The statistical accuracy of the e^+e^- -data is not yet sufficient for determining also σ_L , σ_T , and σ_I . We expect such measurements in the near future with higher statistics data coming from PETRA and PEP. These cross sections σ_L , σ_T , and σ_I are useful to test the spin structure of the $e^+e^- \rightarrow q\bar{q}g$ matrix element, to measure the spin of the gluon or to obtain independent measurements of the quark-gluon coupling constant. For the latter it is essential to know these cross sections at least up to order α_s^2 since the coupling can uniquely be defined through renormalization only in higher order. The cross section σ_{U+L} has already been calculated up to this order [4]. These calculations have shown that it is possible to define the 3-jet cross section σ_{U+L} in such a way that it is infrared finite up to order α_s^2 [5].

In an earlier paper [6] we have calculated the virtual α_s^2 contributions to the longitudinal cross section σ_L for $e^+e^- \rightarrow q\bar{q}g$. They are infrared singular. In this paper we describe the calculation of the real α_s^2 contributions to the 3-jet cross

section σ_L in order to get the infrared finite cross section which can be compared to experiment.

In Sect. 2 we collect the Feynman diagrams which contribute up to order α_s^2 and give the basic formula from which σ_L is calculated. The method for calculating the real contributions is described in Sect. 3. The results are infrared divergent as are the virtual contributions which are taken over from [6]. The sum of these two contributions is finite. It gives us the final formulas for the longitudinal part of $e^+e^- \rightarrow q\bar{q}g$ which are collected in Sect. 4. To point out some universal features with respect to the polarization of the virtual photon we include also the formulas for σ_{U+L} calculated earlier [4].

2. Higher Order Corrections to $e^+e^- \rightarrow q\bar{q}g$

The diagrams contributing to

$$e^+(p_+) + e^-(p_-) \rightarrow q(p_1) + \bar{q}(p_2) + g(p_3) \tag{2.1}$$

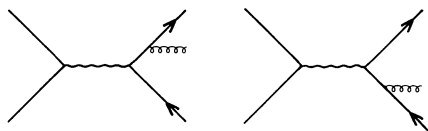
(the symbols in brackets denote the momenta of the particles in the initial and final state respectively) in order α_s^2 are shown in Fig. 2a (the virtual corrections). In Fig. 2b are the diagrams for $e^+e^- \rightarrow q\bar{q}gg$ and $e^+e^- \rightarrow q\bar{q}q\bar{q}$ which contribute to 3 jets in the case when two of the four partons ($qg, \bar{q}g, gg$ etc.) are degenerate. Then the cross section for $e^+e^- \rightarrow 3$ jets in order α_s^2 is obtained by multiplying the diagrams in Fig. 2a with the lowest order diagrams in Fig. 1 and adding the product of the diagrams in Fig. 2b integrated over the 3-jet region of the 4-particle phase space.

The higher order diagrams in Fig. 2 have UV as well as IR divergences. We regulate them by going to $4 - 2\epsilon$ spacetime dimensions [7]. After renormalization the sum of virtual and real contributions is finite.

The cross section for the process (2.1) is ($q = p_+ + p_-$)

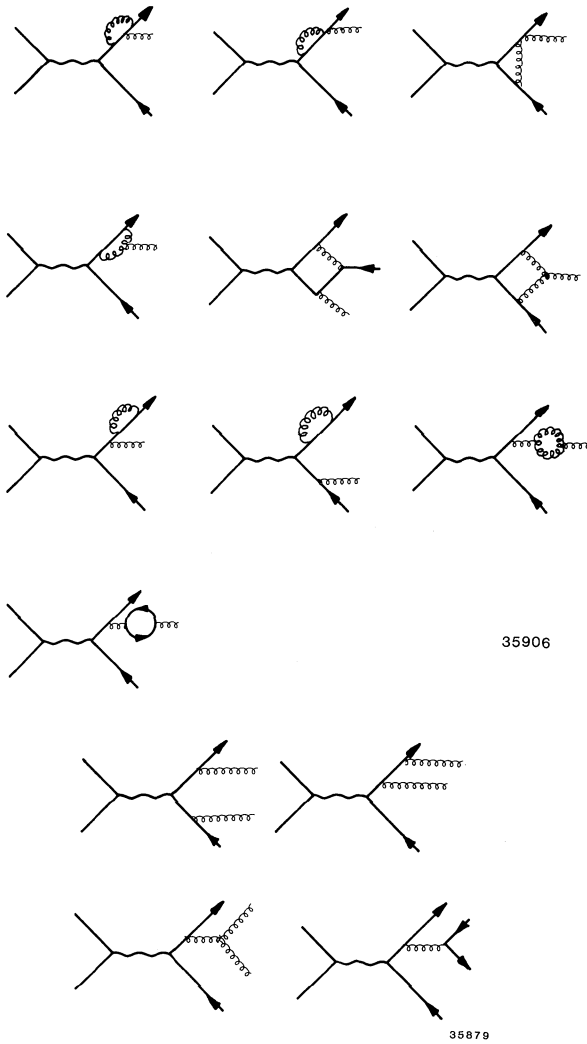
$$d\sigma = \frac{e^4}{2q^6} L^{\mu\nu} H_{\mu\nu} PS^{(3)}, \tag{2.2}$$

where $PS^{(3)}$ is the 3-particle phase space in $4 - 2\epsilon$ dimensions. $L_{\mu\nu}$ is the lepton tensor and $H_{\mu\nu}$ is the hadron tensor, where final spin, colour and flavour together with the quark charge factors are averaged out. Because of current conservation, $q^\mu H_{\mu\nu} = 0$, $H_{\mu\nu}$ in general depends on five structure functions. They can be obtained by expanding $L_{\mu\nu}$ into products of polarization vectors of the incoming virtual photon: $\epsilon_\mu^\pm = 1/\sqrt{2}(0, \mp 1, -i, 0)$ for transverse polarization and $\epsilon^{(0)} = (0, 0, 0, 1)$ for longitudinal polarization in the system $\mathbf{q} = 0$ and then specifying the z -direction in this system. Longitudinal cross sections σ_L are obtained by substituting $\frac{q^2}{3} \epsilon_\mu^{(0)} \epsilon_\nu^{(0)}$



35898

Fig. 1



35906

35879

Fig. 2a and b

for $L_{\mu\nu}$ in (2.2). We have calculated $\sigma_L^{(1)}$ with z -axis parallel to \mathbf{p}_1 and $\sigma_L^{(3)}$ with z -axis parallel to \mathbf{p}_3 . $\sigma_L^{(2)}$ with $z \parallel \mathbf{p}_2$ follows from $\sigma_L^{(1)}$ by interchanging $p_1 \leftrightarrow p_2$. Since $\varepsilon_\mu^{(0)} = p_{i\mu}/p_{i0} - q_\mu/q_0$ ($i=1, 3$) one has to calculate effectively $H_{\mu\nu} p_i^\mu p_i^\nu / p_{i0}^2$ with $i=1, 3$. The total cross section $\sigma_{U+L} = \sigma_U + \sigma_L$ is obtained by integrating over angles

$$\int L_{\mu\nu} \frac{d\Omega}{4\pi} = \frac{q^2}{3} (-g_{\mu\nu} + q_\mu q_\nu / q^2), \tag{2.3}$$

where

$$L_{\mu\nu} = p_{+\mu} p_{-\nu} + p_{-\mu} p_{+\nu} - q^2 / 2 g_{\mu\nu}. \tag{2.4}$$

3. Virtual and Real Corrections

All traces were calculated with the help of REDUCE [8] in $4 - 2\varepsilon$ dimensions. The sum of all graphs, either virtual (see Fig. 2a) or real (see Fig. 2b) consists of four distinct classes: (a) planar QED type graphs with (colour) group weight C_F^2 , (b) non-planar QED type graphs with group weight $C_F(C_F - N_c/2)$, (c) QCD type graphs involving the three gluon vertex with group weight $C_F N_c$ and (d) graphs having a closed fermion loop with group weight $C_F \frac{N_f}{2}$. Here N_f is the number of flavours and $C_F = \frac{4}{3}$, $N_c = 3$ and $T_r = \frac{N_f}{2}$ are the Casimir operators. We used the variables

$$y_{ij} = 2p_i p_j / q^2, \quad (3.1)$$

$$y_{ijk} = y_{ij} + y_{jk} + y_{ik}, \quad i < j < k. \quad (3.2)$$

The calculation of the virtual contributions to $e^+ e^- \rightarrow q\bar{q}g$ using the Gegenbauer expansion method has been described in detail in [6]. The result can be written in the following form

$$\frac{d^2 \sigma_A}{dy_{13} dy_{23}} = \sigma^{(2)} \frac{\alpha_s(\mu^2)}{2\pi} C_F \left(\frac{4\pi\mu^2}{q^2} \right)^\varepsilon \frac{\theta(1 - y_{13} - y_{23} - y_{12})}{\Gamma(2 - \varepsilon)} \cdot (y_{13} y_{23} (1 - y_{13} - y_{23}))^{-\varepsilon} T_A^{\text{virtual}}. \quad (3.3)$$

Here

$$\sigma^{(2)} = \sigma_0 \left(\frac{4\pi\mu^2}{q^2} \right)^\varepsilon \frac{\Gamma(2 - \varepsilon)}{\Gamma(2 - 2\varepsilon)}, \quad \sigma_0 = \frac{4\pi\alpha^2}{3q^2} N_c \sum_{i=1}^{N_f} Q_i^2 \quad (3.4)$$

is the cross section for $q\bar{q}$ production in lowest order in $4 - 2\varepsilon$ dimensions. μ is an arbitrary parameter to define the coupling constant in such a way that it is dimensionless for arbitrary ε . The index A stands for $U + L$, L_1 or L_3 . T_A^{virtual} is written as

$$T_A^{\text{virtual}} = \frac{\Gamma(1 - \varepsilon)}{\Gamma(1 - 2\varepsilon)} \left(\frac{4\pi\mu^2}{q^2} \right)^\varepsilon \frac{\alpha_s(\mu^2)}{2\pi} B_A(y_{13}, y_{23}) C_F \cdot \left\{ C_F T_A^{\text{Cvirtual}} + \frac{N_c}{2} T_A^{\text{Nvirtual}} + \left(\frac{N_f}{3} - \frac{11}{6} N_c \right) T_A^{\text{ct}} \right\}. \quad (3.5)$$

We understand T_A to contain the renormalization counterterm

$$T_A^{\text{ct}} = 1/\varepsilon \quad (3.6)$$

in the \overline{MS} renormalization scheme [9]. B_A stands for the 3-jet distributions to order α_s :

$$\begin{aligned} B_{U+L}(y_{13}, y_{23}) &= (1 - \varepsilon) \left(\frac{y_{13}}{y_{23}} + \frac{y_{23}}{y_{13}} \right) + \frac{2y_{12}}{y_{13} y_{23}} - 2\varepsilon, \\ B_{L_1}(y_{13}, y_{23}) &= 2(1 - \varepsilon) \frac{y_{12}}{(1 - y_{23})^2}, \\ B_{L_3}(y_{13}, y_{23}) &= 4 \frac{y_{12}}{(1 - y_{12})^2}. \end{aligned} \quad (3.7)$$

The explicit formulas for $T_A^{C,\text{virtual}}$ and $T_A^{N,\text{virtual}}$ are rather lengthy and will not be given here. They can be looked up in our earlier work [6] and can be reconstructed from the final formulas for the cross section in (4.1). The singular pieces of $T_A^{C,\text{virtual}}$ and $T_A^{N,\text{virtual}}$ are rather simple and they are identical for $A=U+L$, L_1 and L_3 :

$$\begin{aligned} T_{A,\text{div}}^{C,\text{virtual}} &= -\frac{2}{\varepsilon^2} + \frac{1}{\varepsilon}(2 \ln y_{12} - 3), \\ T_{N,\text{div}}^{N,\text{virtual}} &= -\frac{2}{\varepsilon^2} + \frac{2}{\varepsilon} \ln(y_{13}y_{23}/y_{12}). \end{aligned} \quad (3.8)$$

The fact that the divergent parts of $T_A^{C,\text{virtual}}$ and $T_A^{N,\text{virtual}}$ are equal for $A=U+L$, L_1 , L_3 , i.e. for the three different polarizations of the photon, is quite remarkable. It would be interesting to know whether this is true in general, i.e. also for the other cross sections σ_T and σ_I which have not been calculated yet. To point out this universal behaviour of the divergent parts is one of the reasons why we have included the total cross section σ_{U+L} as one of the cases in (3.3) and (3.5), although it was reported before.

We now come to the main part of this paper, the calculation of the real contributions to σ_{L_1} and σ_{L_3} . In order to produce physical cross sections one must add to the virtual contributions, given above, the infrared and collinear divergent parts of the four-parton cross sections $d\sigma_{q\bar{q}g\bar{g}}$ and $d\sigma_{q\bar{q}q\bar{q}}$ integrated over a small phase space region which includes the singularities. To define this region one needs parameters to parametrize the boundary of the region inside which two partons are considered to be irresolvable, i.e. being one jet. For this we use an invariant mass constraint. The partons i and j are said to be irresolvable if the invariant mass squared $(p_i + p_j)^2 = 2p_i p_j$ is less than yq^2 (all partons being massless). This boundary has been used also for defining $d\sigma_{U+L}(y)$ in [4, second reference]. It has the advantage that it depends only on one parameter which makes it easier to study the dependence of $d\sigma_{3\text{-jet}}(y)$ on the boundary. We calculate $d\sigma_{3\text{-jet}}(y)$ only up to terms of order 1, i.e. we neglect term of order $y \ln y$ and higher. Therefore our results are applicable only for small $y \lesssim 0.05$ [1, 4]. To obtain these dominant terms we need only the most singular parts of the 4-parton matrix elements $\sim y_{ij}^{-1}$ which we take from our earlier work [4]. Of course, these matrix elements and the 4-parton phase space must be calculated in $4-2\varepsilon$ dimensions.

For the case that we integrate over the singularity y_{13}^{-1} , i.e. that parton 1 and 3 form one jet, the 4-parton phase space is [5]

$$\begin{aligned} PS^{(4)} &= \frac{q^4}{2^{11}\pi^3} \frac{S}{\Gamma(1-\varepsilon)\Gamma(2-2\varepsilon)} \left(\frac{4\pi}{q^2}\right)^{3\varepsilon} \\ &\cdot \int dy_{123} dy_{134} dy_{13} (y_{123}y_{134} - y_{13})^{-\varepsilon} \\ &\cdot (y_{13} + 1 - y_{123} - y_{134})^{-\varepsilon} y_{13}^{-\varepsilon} \theta(y_{13}) \\ &\cdot \theta(y_{123}y_{134} - y_{13}) \theta(y_{13} + 1 - y_{123} - y_{134}) \\ &\cdot \int_0^1 dv v^{-\varepsilon} (1-v)^{-\varepsilon} \frac{1}{N_{\theta'}} \int_0^\pi d\theta' \sin^{-2\varepsilon}\theta'. \end{aligned} \quad (3.9)$$

S is a statistical factor, $N_{\theta'}$ is the normalization for the θ' integration. For defining the angles we take the system $z \parallel \mathbf{p}_2$ and $\mathbf{p}_1 + \mathbf{p}_3 = 0$. Then θ and θ' are the polar

angles of \mathbf{p}_1 in this system and

$$v = \frac{1}{2}(1 - \cos\theta) = 1 - \frac{y_{23}}{y_{123}}. \tag{3.10}$$

It appears that this coordinate system is very convenient for doing the rather complicated integrations of the singular terms over the 3-jet region bounded by y . Since the longitudinal cross sections $d\sigma_{L_1}$ and $d\sigma_{L_3}$ are obtained from invariant quantities $H_{\mu\nu}p_1^\mu p_1^\nu$ and $H_{\mu\nu}p_3^\mu p_3^\nu$ respectively the choice of the coordinate system does not matter.

When calculating the contributions to $H_{\mu\nu}p_1^\mu p_1^\nu$ and $H_{\mu\nu}p_3^\mu p_3^\nu$ one must be careful concerning the correct definition of the labels “1” and “3”. Integrating over the singularity $1/y_{13}$ means that $p_3 \rightarrow 0$ or $p_3 \parallel p_1$. Then the corresponding 3-jet momenta are $p_I = p_1 + p_3$, $p_{II} = p_2$, and $p_{III} = p_4$, so that actually one has to calculate $H_{\mu\nu}p_I^\mu p_I^\nu = H_{\mu\nu}(p_1 + p_3)^\mu (p_1 + p_3)^\nu = v$ etc. Only with this choice of 3-jet momenta for defining $d\sigma_{L_1}$ and $d\sigma_{L_3}$ one can achieve consistency, i.e. the cancellation of the $1/\varepsilon^2$ and $1/\varepsilon$ singularities. In the end all contributions are proportional to $B_A(y_{I\text{III}}, y_{\text{III}})$ as they should.

Before presenting the results we make a few remarks concerning the region of integration in (3.7). For the graphs of type (c) with a gluon loop and the graphs of type (d) the singularity is $1/y_{34}$ instead of $1/y_{13}$. Then one uses the analogue of the phase space formula (3.9) in the system $\mathbf{p}_3 + \mathbf{p}_4 = 0$ and integrates over $0 \leq y_{34} \leq y$. Outside the 2-jet region $y \ll y_{134}, y_{234}$, and the integrations are rather simple. For the other graphs the v -integration is somewhat complicated, because one has singularities $1/y_{13}$ and $1/y_{23}$ which must be considered together. To avoid double counting in the infrared region, $p_3 \rightarrow 0$, one integrates the $1/y_{13}$ terms over the region

$$2 \int_0^1 dv - \int_{1-y/y_{\text{III}}}^1 dv, \tag{3.11}$$

which then accounts correctly for the $1/y_{23}$ contribution.

After having done the θ' -integration we obtain the following expression for the integrand,

$$\begin{aligned} \text{Integrand} = B_A(y_{\text{I\text{III}}, y_{\text{III}}}) \left\{ C_F \frac{1}{y_{13}} \left(\frac{2v}{1-v} + (1-\varepsilon)(1-v) \right) \right. \\ \left. + N_c \frac{2}{y_{34}} \left(\frac{v}{1-v} + v(1-v) \right) + \frac{N_f}{2} \frac{1}{y_{34}} \frac{v^2 + (1-v)^2 - \varepsilon}{1-\varepsilon} \right\}. \tag{3.12} \end{aligned}$$

A stands for $U + L, L_1$ and L_3 . $y_{\text{I\text{III}}}$ and y_{III} are the 3-jet variables. Equation (3.12) must be integrated over (3.11) and $0 \leq y_{13} \leq y$ in the case of the $1/y_{13}$ singular part and over the analogous regions in the case of the $1/y_{34}$ singular piece. It is remarkable that the curly bracket in (3.12) is universal for $A = U + L, L_1$ and L_3 . For graphs of type (a) and (b), which do not depend on θ' this is obvious. In this case one encounters in the original expression within the traces always the following product

$$\dots \bar{v}(p_1) \not{\epsilon}(p_1 + p_3) \dots \tag{3.13}$$

where ε is the polarization vector of the gluon which has momentum p_3 . We decompose $p_3 = p_3^\parallel + p_3^\perp$ with respect to p_1 , i.e. $p_3^\parallel(p_3^\perp)$ is in the direction of (perpendicular to) p_1 . p_3^\perp is small since parton 1 and 3 are assumed to form one jet

and can be neglected. Then the expression (3.13) goes over into

$$\dots \bar{v}(p_1) \frac{\not{\epsilon}(\not{p}_1 + \not{p}_3)}{2p_1 p_3} \dots = \frac{2\epsilon(p_1 + p_3)}{2p_1 p_3} \dots \bar{v}(p_1) \dots, \quad (3.14)$$

so that (3.13) is reduced to a contribution equal to the lowest order diagrams in Fig. 1 multiplied by a universal function which is independent of the virtual photon polarization. These arguments do not go through for graphs of type (c) and (d). Indeed there one finds that the θ' -dependence of the integrand depends on A . Nevertheless we find the universal factor in (3.12) after integrating over θ' !

The final result is written again in the form (3.3)–(3.5) with “virtual” to be replaced by “real” and T_A^{ct} replaced by $T_A^{N_f N_c \text{real}}$. Instead of the indices I, II, III to label the 3-jet variables we use again 1, 2, 3. Then we obtain

$$\begin{aligned} T_A^{C \text{real}} &= \frac{2}{\epsilon^2} - \frac{1}{\epsilon} (2 \ln y_{12} - 3) + 7 - 4\zeta_2 - 2 \ln^2 y \\ &\quad - 3 \ln y + 4 \ln y \ln y_{12} - \ln^2 y_{12}, \\ T_A^{N \text{real}} &= \frac{2}{\epsilon^2} - \frac{2}{\epsilon} \ln(y_{13} y_{23} / y_{12}) + \frac{4}{3} - 4\zeta_2 - \ln^2 y_{13} - \ln^2 y_{23} \\ &\quad + \ln^2 y_{12} - 2 \ln^2 y + 4 \ln y \ln y_{13} + 4 \ln y \ln y_{23} - 4 \ln y \ln y_{12}, \\ T_A^{N_f N_c \text{real}} &= -\frac{1}{\epsilon} - \frac{5}{3} + \ln y. \end{aligned} \quad (3.15)$$

This completes the calculation of the real contributions with the invariant mass constraint y .

4. Cross Sections

Adding (3.15) to (3.5) it is evident from (3.6) and (3.8) that the infrared and collinear singularities proportional to ϵ^{-2} and ϵ^{-1} cancel. The remainder in the sum gives the 3-jet cross sections for the three polarizations $A = U + L, L_1,$ and L_3 . They are written in the following form in which the lowest order contribution is also included:

$$\begin{aligned} \frac{d^2 \sigma_A}{dy_{13} dy_{23}} &= \sigma_0 \frac{\alpha_s(q^2)}{2\pi} C_F \theta(1 - y_{13} - y_{23}) B_A(y_{13}, y_{23}) \\ &\quad \cdot \left[1 + \frac{\alpha_s(q^2)}{2\pi} \left(C_F T_A^C + \frac{N_c}{2} T_A^N \right) + \left(\frac{N_f}{3} - \frac{11}{6} N_c \right) T_A^{N_f N_c} \right], \end{aligned} \quad (4.1)$$

where

$$\begin{aligned} T_A^C &= -1 + \frac{2}{3} \pi^2 - 2 \ln^2 y_{12} - 2 \ln^2 y + 4 \ln y \ln y_{12} - 3 \ln y + h_A, \\ T_A^N &= \frac{4}{3} + \frac{1}{3} \pi^2 + 2 \ln^2 y_{12} - 2 \ln^2 y_{13} - 2 \ln^2 y_{23} - 2r(y_{13}, y_{23}) \\ &\quad - 2 \ln^2 y + 4 \ln y \ln(y_{13} y_{23} / y_{12}) + g_A, \\ T_A^{N_f N_c} &= -\frac{5}{3} + \ln y, \end{aligned} \quad (4.2)$$

and the functions h_A and g_A appearing in (4.2) have the following form:

$$\begin{aligned} h_{U+L} &= \hat{g}(y_{13}, y_{23}) / B_{U+L}(y_{13}, y_{23}), \\ h_{L_1} &= -\frac{2}{3} \pi^2 + 2 \ln y_{23} + \frac{2 y_{13}}{y_{13} + y_{23}} + 2 \ln y_{12} \left(\frac{y_{13}}{y_{13} + y_{23}} + \frac{y_{12} y_{23}}{(y_{13} + y_{23})^2} \right) \end{aligned}$$

$$\begin{aligned}
& -2r(y_{12}, y_{13}) + 2\frac{y_{12}}{y_{13}}r(y_{12}, y_{23}), \\
h_{L_3} = & -\frac{2}{3}\pi^2 + 2\ln y_{12} + \frac{y_{13} + y_{23}}{2y_{12}} - \frac{y_{13}^2}{2y_{12}(y_{12} + y_{13})} - \frac{y_{23}^2}{2y_{12}(y_{12} + y_{23})} \\
& + \frac{1}{2}\ln y_{13} \left(\frac{y_{13}y_{23}}{(y_{12} + y_{23})^2} + \frac{2y_{23}}{y_{12} + y_{23}} \right) + \frac{1}{2}\ln y_{23} \left(\frac{y_{13}y_{23}}{(y_{12} + y_{13})^2} + \frac{2y_{13}}{y_{12} + y_{13}} \right) \\
& - r(y_{12}, y_{13}) - r(y_{12}, y_{23}), \\
g_{U+L} = & (\tilde{g}(y_{13}, y_{23}) - \hat{g}(y_{13}, y_{23})) / B_{U+L}(y_{13}, y_{23}), \\
g_{L_1} = & -\frac{1}{3}\pi^2 + 1 - \frac{2y_{13}}{y_{13} + y_{23}} - 2\ln y_{12} \left(\frac{y_{13}}{y_{13} + y_{23}} + \frac{y_{12}y_{13}}{(y_{13} + y_{23})^2} \right) \\
& + 2r(y_{12}, y_{13}) - 2\frac{y_{12}}{y_{13}}r(y_{12}, y_{23}), \\
g_{L_3} = & -\frac{1}{3}\pi^2 - 2\ln y_{12} + r(y_{12}, y_{13}) + r(y_{12}, y_{23}) - \frac{y_{13}}{y_{12} + y_{23}} \ln y_{13} \\
& - \frac{y_{23}}{y_{12} + y_{13}} \ln y_{23},
\end{aligned} \tag{4.3}$$

with $r(x, y)$, $\hat{g}(y_{13}, y_{23})$ and $\tilde{g}(y_{13}, y_{23})$ defined as in [6]:

$$r(x, y) = \ln x \ln y - \ln x \ln(1-x) - \ln y \ln(1-y) - L_2(x) - L_2(y) + \frac{1}{6}\pi^2,$$

$$\begin{aligned}
\hat{g}(y_{13}, y_{23}) = & 4\ln y_{12} \left[\frac{2y_{12}}{y_{13} + y_{23}} + \frac{y_{12}^2}{(y_{13} + y_{23})^2} \right] \\
& + \ln y_{13} \left[\frac{4y_{12}}{y_{12} + y_{23}} + \frac{2y_{13}}{y_{12} + y_{23}} - \frac{y_{13}y_{23}}{(y_{12} + y_{23})^2} \right] \\
& + \ln y_{23} \left[\frac{4y_{12}}{y_{12} + y_{13}} + \frac{2y_{23}}{y_{12} + y_{13}} - \frac{y_{13}y_{23}}{(y_{12} + y_{23})^2} \right] \\
& - 2r(y_{12}, y_{13}) \frac{y_{12}^2 + (y_{12} + y_{23})^2}{y_{13}y_{23}} \\
& - 2r(y_{12}, y_{23}) \frac{y_{12}^2 + (y_{12} + y_{13})^2}{y_{13}y_{23}} + \frac{y_{12}}{y_{12} + y_{13}} \\
& + \frac{y_{12}}{y_{12} + y_{23}} + \frac{4y_{12}}{y_{13} + y_{23}} - \frac{y_{12}}{y_{13}} - \frac{y_{12}}{y_{23}} - \frac{y_{13}}{y_{23}} - \frac{y_{23}}{y_{13}}, \tag{4.4}
\end{aligned}$$

$$\begin{aligned}
\tilde{g}(y_{13}, y_{23}) = & \ln y_{13} \left[4\frac{y_{12} + y_{13}}{y_{12} + y_{23}} - \frac{y_{13}y_{23}}{(y_{12} + y_{23})^2} \right] \\
& + \ln y_{23} \left[4\frac{y_{12} + y_{23}}{y_{12} + y_{13}} - \frac{y_{13}y_{23}}{(y_{12} + y_{13})^2} \right] \\
& + \frac{y_{12}}{y_{12} + y_{13}} + \frac{y_{12}}{y_{12} + y_{23}} + \frac{y_{12}}{y_{13}} + \frac{y_{12}}{y_{23}} + \frac{y_{13}}{y_{23}} + \frac{y_{23}}{y_{13}}.
\end{aligned}$$

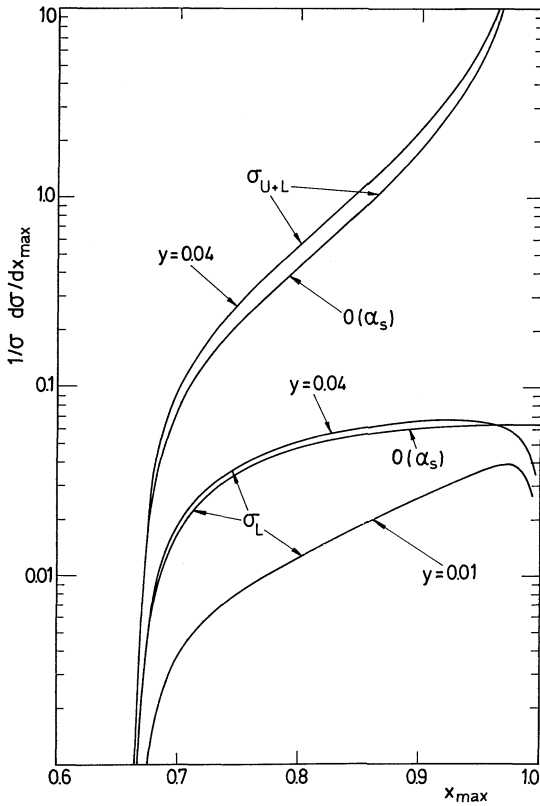


Fig. 3. Three-jet cross sections $1/\sigma d\sigma_{U+L}/dx_{\max}$ and $1/\sigma d\sigma_L/dx_{\max}$ for $y=0.04$ and $y=0.01$ together with the Born cross section ($O(\alpha_s)$) as a function of x_{\max} for $\alpha_s=0.16$

These formulas contain all results which are known up to now about 3-jet cross sections with invariant mass resolution. The result for $d^2\sigma_{U+L}$ agrees with our earlier calculations [4]. We have included it here since it makes it easier to program all three cross sections simultaneously when used for analysing experimental data.

In order to get an idea about the amount of corrections originating from the higher order terms we have plotted in Fig. 3 $1/\sigma d\sigma_L/dx_{\max}$ as a function of x_{\max} for $y=0.04$ and $y=0.01$ together with the $O(\alpha_s)$ curve. x_{\max} is the 3-parton thrust equal to the maximum of x_1 , x_2 , and x_3 where $x_i = 1 - y_{jk}$ (ijk cyclic). We have $N_f=5$ and $\alpha_s=0.16$, which is a realistic value obtained from analysis of experimental distributions of σ_{U+L} with $O(\alpha_s^2)$ corrections included [2]. We see that for $y=0.04$ the $O(\alpha_s^2)$ corrections to the x_{\max} distribution are quite small. In average they amount to an increase of 6% if compared to the $O(\alpha_s)$ curve. The larger deviation above $x_{\max}=0.95$ is in the two-jet region and is caused by the cut-off $y=0.04$. For $y=0.01$ the corrections are very large. But $y=0.01$ lies outside the perturbative region as was already observed in connection with σ_{U+L} [4]. For comparison the x_{\max} distribution $1/\sigma d\sigma_{U+L}/dx_{\max}$ is also shown for $y=0.04$ and in

$O(\alpha_s)$. Here the correction caused by the $O(\alpha_s^2)$ terms are somewhat larger, near 25% in average.

The results given here are valid only as long as terms $O(y)$ can be neglected. So one must choose y small enough for using these formulas. In case one wants results for larger y 's where our approximation might be questionable one always can choose first a small y and correct for the difference numerically by adding the 4-jet contribution in the desired y bin with two partons lying in this bin averaged over.

Appendix

In our earlier paper [6] we discovered the following printing errors: In (4.10) the second line reads

$$\frac{1}{\epsilon}(2\ln y_{12} - 3) - 8 + \frac{2}{3}\pi^2 - \ln^2 y_{12}.$$

In (4.19) I_2 and I_3 are:

$$I_2 = N_c \left(\ln^2 \frac{y}{y_{12}} - \ln^2 \frac{y}{y_{13}} - \ln^2 \frac{y}{y_{23}} - r(y_{13}, y_{23}) - \frac{11}{6} \ln y + \frac{67}{18} + \frac{1}{6}\pi^2 - \frac{y}{y_{12}} \ln \frac{y^2}{y_{12}} + \frac{y}{y_{13}} \ln \frac{y^2}{y_{13}} + \frac{y}{y_{23}} \ln \frac{y^2}{y_{23}} \right),$$

$$I_3 = \frac{N_f}{2} \left(\frac{2}{3} \ln y - \frac{10}{9} \right).$$

References

1. Kramer, G.: Theory of jets in electron-positron annihilation. Springer tracts in modern physics, Vol. 102. Berlin, Heidelberg, New York: Springer 1984
2. Wolf, G.: The determination of α_s in e^+e^- annihilation. Talk presented at the XIVth Intern. Symposium on multiparticle dynamics. Lake Tahoe, CA (June 1983) DESY-report 83-096 (1983)
3. Kramer, G., Schierholz, G., Willrodt, J.: QCD predictions for jets in e^+e^- annihilation: angular correlations and asymmetries. Phys. Lett. **78 B**, 249 (1978), Erratum Phys. Lett. **80 B**, 433 (1979)
4. Fabricius, K., Kramer, G., Schierholz, G., Schmitt, I.: Higher order perturbative QCD calculation of jet cross sections in e^+e^- annihilation. Z. Physik **C 11**, 315 (1982)
Gutbrod, F., Kramer, G., Schierholz, G.: Higher order QCD corrections to the three-jet cross section: bare versus dressed jets. Z. Physik **C 21**, 235 (1984)
5. For the infrared finiteness of the sum of 3- and 4-jet cross section in the limit of zero jet resolution see: Ellis, R.K., Ross, D.A., Terrano, A.E.: The perturbative calculation of jet structure in e^+e^- annihilation. Nucl. Phys. **B 178**, 421 (1982)
6. Lampe, B., Kramer, G.: Application of Gegenbauer integration method to e^+e^- annihilation. Physica Scripta **28**, 585 (1983). Some misprints in this paper are corrected in the appendix
7. 't Hooft, G., Veltman, M.: Regularization and renormalization of gauge fields. Nucl. Phys. **B 44**, 189 (1972)
8. Hearn, A.C.: REDUCE 2, a system and language for algebraic manipulation. Comm. ACM **14**, 511 (1971)
9. 't Hooft, G., Veltman, M.: Dimensional regularization and the renormalization group. Nucl. Phys. **B 61**, 455 (1973)

Communicated by G. Mack

Received August 30, 1984